Biomass Conversion and Biorefinery
https://doi.org/10.1007/s13399-024-05278-x

ORIGINAL ARTICLE

# Understanding the material properties of alkali-treated lignocellulose fiber obtained from high-altitude Lokta bushes

**Girja Mani Aryal[1] · Krisha Prasad Kandel[1] · Menuka Adhikari[2] · Jianna Evans[2] · Hisila Dangol[1] · Madan Poudel[1] · Sushil Pokharel[1] · Ramdeep Shrestha[1] · Bhoj Gautam[2] · Bhanu Bhakta Neupane[1]**

Received: 3 October 2023 / Revised: 27 December 2023 / Accepted: 1 January 2024


## Abstract

Lignocellulose fiber obtained from high-altitude plant species *Daphne bholua* and *Daphne papyracea*, locally named Lokta bushes, is used in Asian regions to fabricate high-quality handmade paper sheets, packaging materials, composites, and paper bills. A systematic study on the material properties of the fiber to explain the performance of Lokta fiber–based materials has not been reported yet. In this study, the physio-chemical properties of untreated and 1%, 3%, 6%, and 9% NaOH (w/v)-treated Lokta fiber were systematically investigated at ambient temperature. The retting efficiency and cellulose content increased with alkali concentration followed by a decrease in lignin, hemicellulose, and extractives. This observation was consistent with the reduction of lignin and hemicellulose characteristics peaks in the FTIR, a reduction of effective fiber bundle width, and an increase in fiber density. High-resolution scanning electron microscope (SEM) images showed that alkali treatment results in significant loss of cementing materials and separation of fiber bundles. Alkali retting also increased the crystallinity index, tensile strength, and thermal stability. The degradation temperature for untreated, 6% NaOH treated, and 9% NaOH treated samples was found to be 325 °C, 343 °C, and 347 °C; respectively. The findings of this study will be important to optimize the end properties of the Lokta fiber–based paper and composite materials.

**Keywords** Lignocellulose biomass · Cellulose · Retting efficiency · Mechanical strength · Fiber density

## 1 Introduction

In recent decades, lignocellulose fibrous biomass obtained from different natural sources has been explored as an alternative material to synthetic fibers. As compared to synthetic fibrous materials, the biomass-based materials offer unique advantages such as lightweight, high specific strength, flexibility, biodegradability, and abundance. Because of these advantages, the natural fiber–reinforced materials are being explored as an alternative material in several sectors, such as health care, textiles, agro-products, and the automobile industry [1–10].

The fibrous biomass can be obtained from various parts of plants, such as roots, bark, leaf, and fruit. The major chemical components in natural fiber are cellulose, hemicellulose, lignin, and pectin. These chemical constituents are found in the primary cell walls of plants. In plant cell walls, semi-crystalline cellulose microfibrils are embedded in a hemicellulose-lignin matrix of varying composition [11–13]. Therefore, raw fiber is considered a composite material.

The quality of the fiber not only depends on the source but also on the processing parameters such as nature of retting agent and concentration, temperature and treatment time, etc. The size of microfibrils, microfibrils angles or orientation, degree of crystallinity, and the chemical composition are the major parameters that determine the overall quality of the fiber bundle [14–16]. On alkali treatment, the cementing materials such as lignin and hemicellulose are removed from the fiber resulting in partial or complete separation of fiber bundles, reduction of width, and increase in aspect ratio. This makes pulping easier for the intended materials such as papers, cardboards, and composites. Under optimized processing conditions, the end properties of fiber

✉ Bhoj Gautam
bgautam@uncfsu.edu

✉ Bhanu Bhakta Neupane
newbhanu@gmail.com

[1] Central Department of Chemistry, Tribhuvan University, Kathmandu 44613, Nepal

[2] Department of Chemistry, Physics and Materials Science, Fayetteville State University, Fayetteville, NC 28301, USA

Published online: 15 January 2024

such as water resistance, thermal and mechanical strength are significantly improved. For example, increase in tensile strength and thermal stability on alkali treatment was reported in *Neuropeltis acuminatas* liana fiber [17], *Megaphrynium macrostachyum* fiber [18], Kenaf fiber [19], Alfa fiber [20], and banana fiber [21]. If natural fiber is intended for cellulose-polymer composite, alkalization or mercerization leads to the formation of mercerized cellulose structure (for example, fiber-OH to fiber-$ONa^+$) so that bonding with polymer increases [3].

Natural fiber obtained from different plant species and bacteria is actively investigated by several researchers throughout the world [5, 12, 22–29]. Most of the studies are focused on extraction, physicochemical, physicomechanical, and thermomechanical characterization. Applications of these fibers in the fabrication of green composite materials are also being explored [2, 11, 30–33]. From a material point perspective, the natural fiber obtained from *Daphne bholua* and *Daphne papyracea*, locally named Lokta bushes, is one of the least studied plant species. The Lokta bushes are distributed in different districts of Nepal and other Asian countries at an altitude of 1600 to 4000 m. In Nepal, bast fiber obtained from Lokta bushes is being used to make handmade Lokta paper, packaging materials, and gifts. Handmade paper is being used in religious books and documents, official documents, packaging, stationary, greeting cards, decorative products, etc. [24, 34–36]. To understand the end applications of materials made from Lokta fiber, it is important to explore fiber properties processed under different conditions. The motivation of this study was to explore several materials properties of raw and alkali-treated Lokta fiber down to microscopic level and explain the observed differences in water absorptivity, thermal, and mechanical properties.

In this study, raw fibrous biomass obtained from Lokta bushes was treated with 1–9% NaOH solution. The change in chemical composition and weight loss was systematically measured. Several important material properties of the untreated and alkali treated samples such as effective fiber bundle width, crystallinity, and thermal stability were explored using optical microscopic, XRD, SEM, and TGA techniques. Finally, variation on end properties such as water absorptivity, thermal stability, and tensile strength with change in alkali concentration were systematically explored and compared with other fiber types.

## 2 Materials and methods

### 2.1 Extraction and alkaline treatment of fibers

Fully matured stems (~45 cm long and 1.5 cm diameter) were cut from Lokta bushes from Annapurna municipality, Myagdi, Nepal (Fig. 1A and B). The stems were brought to the lab and soaked in distilled water for 60 min. The bark region of the stem (area b, Fig. 1C) was mechanically peeled, and the outer cuticular layer (area a, Fig. 1C) was removed with a stainless steel knife. The fiber bundles were washed with distilled water to remove the surface impurities and sun dried to remove the moisture (Fig. 1D).

The extracted raw Lokta fiber (4–5 cm long and 0.5–1.5 mm wide) was treated with 1%, 3%, 6%, and 9% (w/v) sodium hydroxide solution at room temperature (24 ± 1 °C) for 1 h. The biomass after treatment was washed with tap water 2–3 times, washed with 0.1N HCl to neutralize residual NaOH on the surface of the fibers [37, 38], rinsed 4–5 times with distilled water, and oven-dried (90 ± 2 °C) for 24 h. The % weight loss or retting efficiency (ε) was calculated as:

$$\varepsilon = 100\left(\frac{W_1 - W_2}{W_1}\right) \tag{1}$$

where, $W_1$ and $W_2$ are the initial and final mass of the fiber, respectively.

### 2.2 Determination of biomass composition and water absorption

The percentage of extractives, cellulose, hemicellulose, lignin, and ash content both in untreated and retted and alkali-treated fiber samples was determined following the literature reported gravimetric methods [12, 37, 39, 40]. The % composition (χ) of each component was calculated as:

$$\chi = 100\left(\frac{a - b}{a}\right) \tag{2}$$

where, $a$ and $b$ are initial and final dry weights of the fibrous biomass, respectively.

Three independent measurements were made for each component, and mean and standard deviation (mean ± SD) were reported.

#### 2.2.1 Determination of extractives

The 2.000 g of oven dried raw fiber along with 200 mL of 190 proof ethyl alcohol (95%) was added to a Soxhlet extraction apparatus. The content was refluxed for 6 h. The extracted solid was filtered through filter paper, dried, and weighed. The initial and final weights of fiber were used extractive content using Eq. 2.

#### 2.2.2 Determination of cellulose

To determine cellulose, 1.000 g of extractive-free fiber was oven-dried at ~ 90 ± 2 °C for 4 h and cooled in non-hygroscopic desiccator, and the sample was treated with 5% NaOH (w/v) for 5 h while keeping fiber mass to alkali solution ratio of 1:30 (w/v). The content was cooled and neutralized with

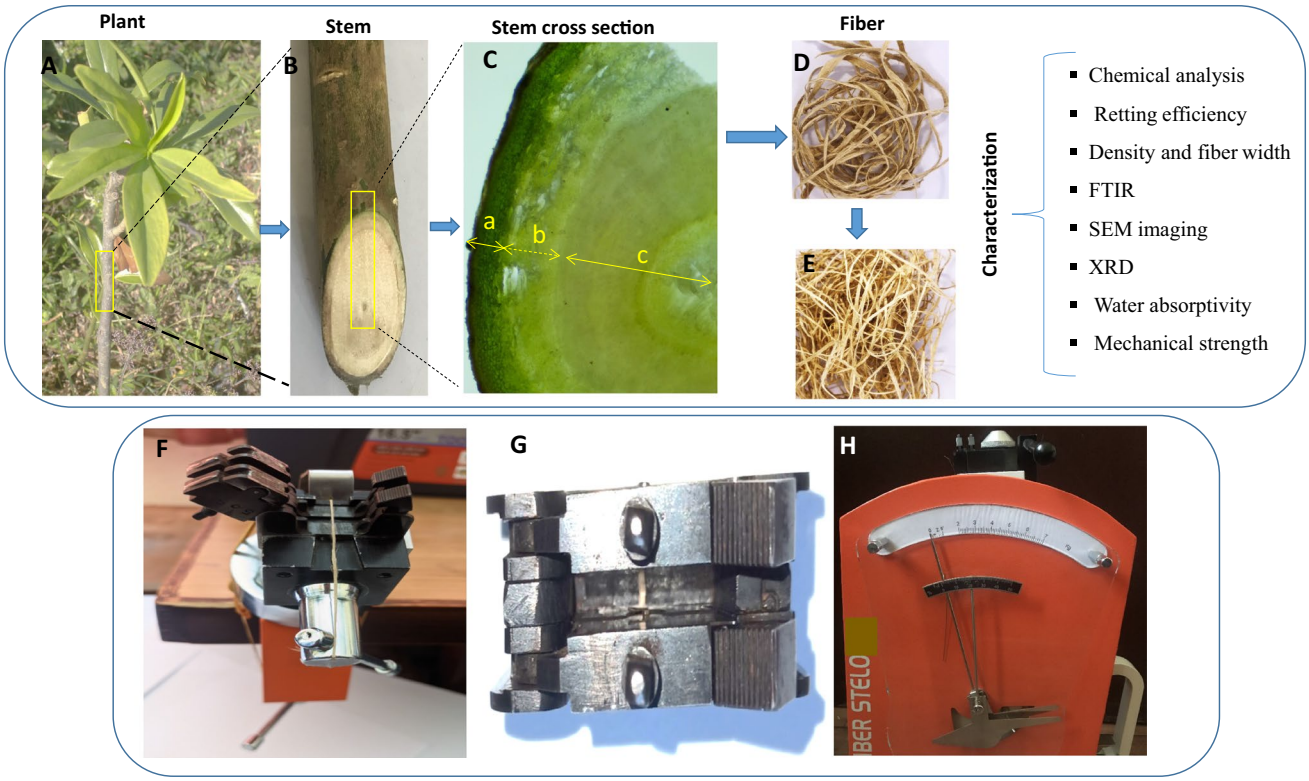


**Fig. 1** Experimental flow chart and mechanical strength testing setup. **A** Lokta plant; **B** freshly cut stem; **C** stem cross section taken with a stereomicroscope: a = cuticular layer, b = bark region, c = woody region; **D** untreated fiber; **E** alkali-treated fiber; **F** A thin fiber bundle ready to mount in Pressley jaw; **G** fiber mounted in Pressley jaw; **H** front view of fiber bundle strength tester showing the load (upper) and % elongation (lower) scales

10% $H_2SO_4$. The residual biomass was washed several times with distilled water and then dried at 90 ± 2 °C until constant weight was obtained. The final and initial weights were used to calculate the cellulose content using Eq. (2).

### 2.2.3 Determination of hemicellulose

To determine the hemicellulose, 1.000 g of extractive free and oven dried sample was boiled in 0.5 M NaOH for 4 h. The content was neutralized after several washings with distilled water, and dried at 90 ± 2 °C till constant weight was obtained. The final and initial weights were used to calculate hemicellulose content.

### 2.2.4 Determination of lignin

Acid insoluble lignin (Klason lignin) was determined following literature reported method [12, 37, 39, 40]. To determine the lignin, 1.000 g of extractive free and oven dried sample (40–50 micron mesh size) was taken in a flask and digested with 15 mL of 72% $H_2SO_4$. The content was carefully stirred 3 h at room temperature, and then around 200 mL of distilled water added and boiled 2 h. The content was cooled to room temperature, and the residue was carefully transferred to a crucible. The residue was washed several times till it becomes acid free (checked with litmus paper). The residue was oven dried at 105 °C till a constant weight was achieved. The fiber and residue were used to get % lignin content.

### 2.2.5 Determination of equilibrium moisture content

To measure the moisture content at ambient condition, 2.000 g of fiber sample was conditioned was oven dried at 90 ± 2 °C for 24 h. The sample was cooled in a non-hygroscopic desiccator and weighed. The difference in the weights before and after drying was used to calculate the moisture content in the fiber. Three independent measurements were made for each sample.

### 2.2.6 Determination of water absorptivity

Fixed weight of fiber bundle was submerged in 50 mL distilled water at room temperature (24 ± 1 °C). The fiber was

taken out at certain time period and weighed. The process was repeated for the intended time period (0–12 days), and % weight gain was calculated from the weight difference [41, 42].

#### 2.2.7 Determination of fiber density and width

The density of cellulose fiber was measured gravimetrically following liquid pyknometer method [43, 44]. Fibers were cut to ~ 5 mm length and dried for 48 h in a non-hygroscopic desiccator ($CaCl_2$ as a desiccant) and impregnated in toluene for around 2 h to remove any microbubbles. The density was then calculated as [43, 44]:

$$\rho = \frac{(m_2 - m_1)\rho_T}{(m_3 - m_1) - (m_4 - m_1)} \quad (3)$$

where, $\rho_T$ is the density of toluene and $m_1$, $m_2$, $m_3$, and $m_4$ are the weight (in grams) of the empty pyknometer, pyknometer with fibers, pyknometer filled with toluene, and pyknometer filled with fiber and toluene solution, respectively.

To determine the fiber width, the fiber bundles were imaged with an optical microscope at magnification of 40 × (Olympus, SZ61, USA). The field of view was calibrated using a high- precision linear calibration grid having least count of 10 µm. The pixel size was converted to a micrometer using image analysis software (ImageJ, NIH, USA) to get fiber width information. Data were reported as the mean values obtained from thirty independent measurements.

### 2.3 Determination of fiber strength

The Lokta fiber samples were preconditioned at 65% RH at 23 ± 2 °C for 24 h following the ASTM test method [45]. To ensure the control measurement condition, fiber bundle obtained from the same region of stem having uniform width (300–350 µm; as examined under microscope) was mounted to the Pressley Jaw assembly gauge length 15 mm (Fig. 1F and G), loaded to the fiber bundle strength tester (Fig. 1H) (TSI instruments, max load 7 kg) and pulled at a constant loading speed of 1 kg/s. The load at which the fiber bundle breaks and the corresponding % elongation was noted. From measured values for breaking load and broken bundle weight (measured at nearest accuracy of 0.0001 g), breaking tenacity (cN/tex) was calculated. The tenacity was converted to ultimate tensile strength or stress using Eq. (4) [46]. Data were reported as the mean values obtained from fifteen independent measurements.

$$S = 10.d.T \quad (4)$$

here, $S$ is the tensile strength (MPa), $d$ is the material density in g $cm^{-3}$, and $T$ is the tenacity (cN/tex).

### 2.4 FTIR, XRD, SEM, and TGA measurements

XRD data were measured in the range of 5–50° at the step size of 0.02° and scan rate of 0.25°/s using an X-ray diffractometer (Rigaku, UK). The X-ray source originating from Cu Kα line (λ = 1.540A°) was used in the measurement.

Scanning electron microscopic images were measured at different magnifications using JEOL JSM-6510LV scanning electron microscope (SEM). The samples were sputter coated with gold (thickness ~ 5 nm) before doing SEM.

The IR spectra were measured in attenuated total reflection (ATR) mode using a Fourier transform infrared spectrometer (ABB Bomen, MB100, Canada). The scan range, spectral resolution, and number of scans were 4000–400 $cm^{-1}$, 4 $cm^{-1}$, and 100, respectively.

The thermo gravimetric analysis (TGA) data were collected using a TG/DTA simultaneous measuring instrument (Shimadzu DTG-60 series) under a nitrogen atmosphere. The sample weight was ~ 10 mg, and fiber size was ~ 3 mm long and 500 µm wide. The temperature range, heating rate, temperature precision, and balance accuracy were 25 to 600 °C, 10 °C/min, ± 2 °C, and 0.1 µg, respectively.

### 2.5 Statistical analysis

The as-measured data were entered and analyzed in Excel spreadsheet to get descriptive statistical parameters such as mean and standard deviation. To find if the mean difference in the mechanical properties is significant, a paired $t$ test at 95% confidence interval was performed and $p$ value was calculated. The level of correlation between two variables was determined from Pearson correlation coefficient ($r$).

## 3 Results and discussion

### 3.1 Weight loss and chemical composition

The % weight loss is a measure of retting efficiency from the lignocellulose biomass on alkali treatment. It depends on the nature of biomass and retting conditions such as concentration of alkali, treatment time, and temperature [12, 19, 47]. As expected, % weight loss increases with alkali concentration (Fig. 2A). Indeed, a strong positive correlation between alkali concentration and % weight loss was found, as indicated by the Pearson correlation coefficient $r = +0.93$. A maximum weight loss of 27.0 ± 1.6% was achieved on 9% alkali treatment.

The weight loss on alkali treatment results from the removal of non-cellulosic and cementing materials from the biomass. To explore this extractive, Klason lignin,

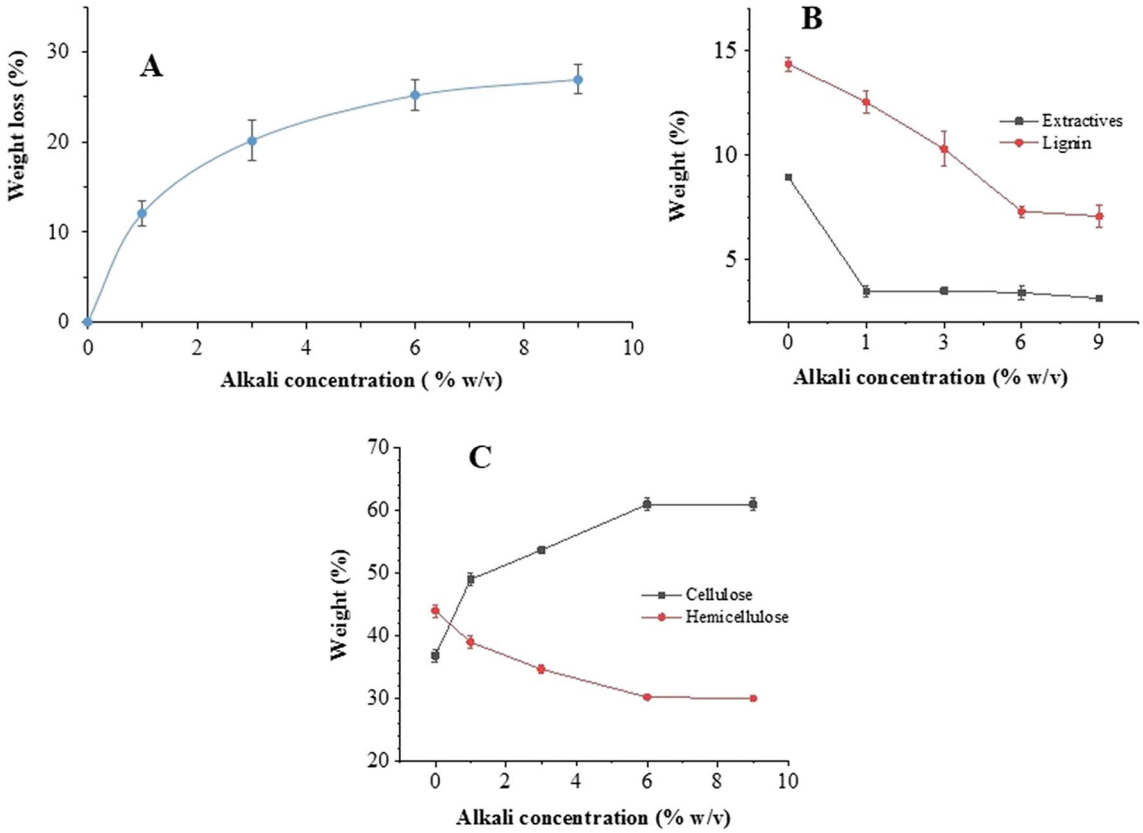


**Fig. 2** The weight loss and chemical composition. **A** Weight loss (%) as a function of alkali concentration. **B** Extractive and lignin content measured as function and alkali concentration. **C** Cellulose and hemicellulose content measured as function and alkali concentration. The error bars in all figures, represent the standard deviation obtained from three independent fiber samples ($n = 3$)

hemicellulose, and cellulose were measured in dry or moisture free samples.

A significant loss in extractive content was observed in alkali-treated samples (Fig. 2B). For example, in a 9% alkali-treated sample ~ 65% extractive loss was found (8.9 ± 0.1 to 3.1 ± 0.0%). Loss of lignin and hemicellulose was also observed in the alkali-treated samples (Fig. 2B and C). In 9% alkali-treated sample, ~ 51.2% lignin loss (14.3 to 7.0%) and 32% hemicellulose loss (44 to 30%) were observed. The cellulose content in untreated, 1%, 3%, 6%, and 9% treated samples was found to be 36.8 ± 1.0, 49.0 ± 1.0, 53.7 ± 1.0, 61.0 ± 1.0, and 61.0 ± 1.0, respectively, suggesting a significant increase in cellulose content on alkali treatment (Fig. 2C). The net increase in cellulose content is due to collective loss of extractive, lignin, and hemicellulose.

Loss of lignin and hemicellulose with increased alkali concentration and the corresponding increase in cellulose content was also reported in Alfa stem fiber [20], *M. oleifera* fruit fibers [48], *Carica papaya* bark fibers [49], and water hyacinth fiber [50], and *Sterculia* fiber [12]. The loss of lignin and hemicellulose could be due to the disruption of specific bonds, for example, hydrogen bonding between cellulose, hemicellulose, and lignin, resulting in partial solubility and washing of the components [51].

**Table 1** Moisture content, density, and fiber width

| Sample type | Moisture content (%) | Density (g $cm^{-3}$) | % decrease in fiber width |
|---|---|---|---|
| Untreated | 13.3 ± 0.2 | 1.11 ± 0.00 | - |
| 1% treated | 11.2 ± 0.1 | 1.17 ± 0.01 | 18.6 ± 3.9 |
| 3% treated | 10.9 ± 0.6 | 1.20 ± 0.01 | 22.7 ± 6.2 |
| 6% treated | 10.4 ± 0.4 | 1.23 ± 0.01 | 25.8 ± 5.2 |
| 9% treated | 9.8 ± 0.5 | 1.38 ± 0.01 | 30.6 ± 5.9 |

## 3.2 Moisture content, density, fiber width, and water absorptivity

Another change in alkali treatment is the decrease in equilibrium moisture content with the increase on alkali concentration (Table 1). For example, in 9% NaOH-treated fiber the equilibrium moisture content decreased by ~ 25% (13.3 to 9.8%). The decreased moisture content could be due to the loss of more hydrophilic components such as extractives and

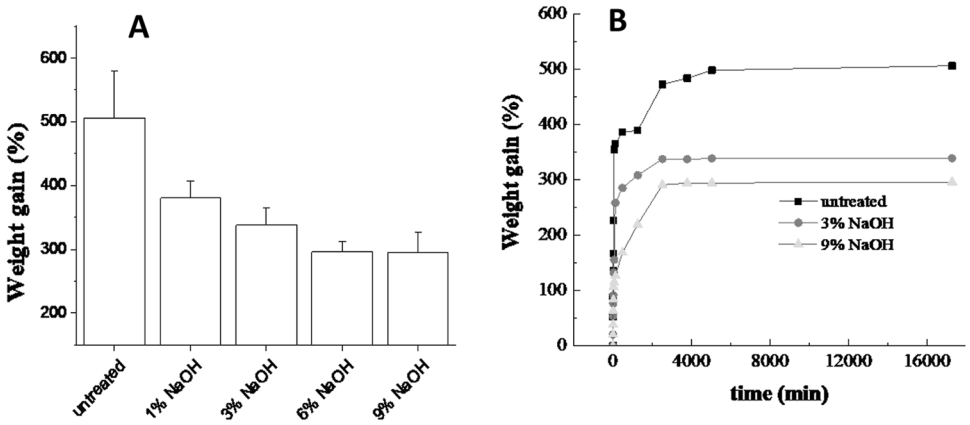


**Fig. 3** Equilibrium water absorption. **A** % weight gain for different samples measured after 12 days. The error bar represents the standard deviation obtained from three independent samples. **B** A typical water absorption kinetics plot for untreated, 3% and 9% NaOH-treated samples

lignin from the fiber bundle. Significant decrease in moisture content on alkali treatment is also reported in other studies; for example, 16.4% decrease (13.4 to 11.2%) is reported for banana fiber treated for 3 h in 10% NaOH [21], ~ 40% decrease (9.7 to 5.8%) in *Carica papaya* bark fibers treated 1 in 5% NaOH [49].

A small but gradual increment in density was observed with an increase in alkali concentration. In fact, density showed strong positive correlation ($r = +0.96$) with alkali concentration. In the 9% alkali-treated sample, a ~ 24% increase in density (1.11 to 1.38 g $cm^{-3}$) was observed (Table 1). In literature studies, depending on alkali concentration and fiber type, density is reported to increase or decrease. An increase in density (by ~ 2.5%) was reported for Kenaf and Hemp fiber treated at or below 10% (w/v), whereas the decrease in density was observed at concentration > 10% [19, 52, 53]. In banana fiber, an increase in density (~ 7–9%) was observed in fiber treated to 10 and 15% alkali [21]. The density increase can be due to the loss of low-density non-cellulosic components or cell wall densification, whereas density decrease could originate due to the cell wall rupture leading to de-polymerization of cellulose chains [19, 21]. In this study, relatively high increase in fiber density could be due to a significant loss of non-cellulosic components from the Lokta fiber.

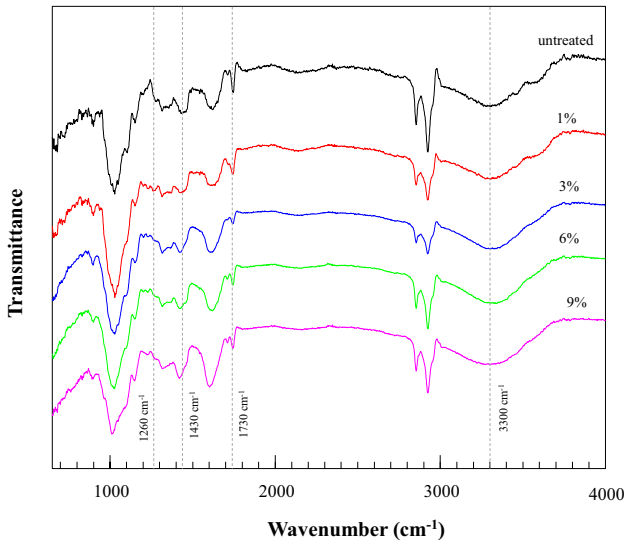


**Fig. 4** FTIR spectra of the fiber samples. For easy compassion, spectra are overlaid vertically. The dotted lines are to indicate the peak position of important frequencies

Another change reported on alkali treatment is a significant decrease in effective fiber bundle width [12, 19, 21]. This is mainly attributed to the loss of non-cellulosic components from the bundle surface. In Lokta fiber, a significant reduction in fiber width was observed in alkali-treated samples (Table 1). The reduction in fiber width on 1%, 3%, 6%, and 9% NaOH treated samples at 95% confidence interval was found to be 18.6 ± 3.9%, 22.7 ± 6.2%, 25.8 ± 5.2%, and 30.6 ± 5.9%; respectively.

The water absroptivity measured in terms of % weight gain in untreated, and 1%, 3%, 6%, and 9% NaOH-treated fiber was found to be 506.2 ± 64.1, 380.8 ± 32.8, 338.7 ± 25.4, 296.0 ± 20.5, and 295.7 ± 42.9%; respectively (Fig. 3A). If cellulose fiber is soaked in water, the hydrogen bond between the fiber chain breaks and new hydrogen bond is formed between fiber-OH groups and water molecules leading to significant weight gain. On alkali treatment, the more hydrophilic components are removed resulting in increased water resistance or decreased water absorptivity [3]. Interestingly, the % weight loss (Fig. 2A) and % weight gain data (Fig. 3A) strongly negatively correlate ($r = -0.98$).

For completeness, the water uptake kinetics curves are also reported for selected samples (Fig. 3B). A typical water absorption kinetic curve, as observed for natural fibers [41, 42, 54], consisting of fast (at short immersion time) and slow water uptake (at longer immersion time) regimes is observed in all the samples.

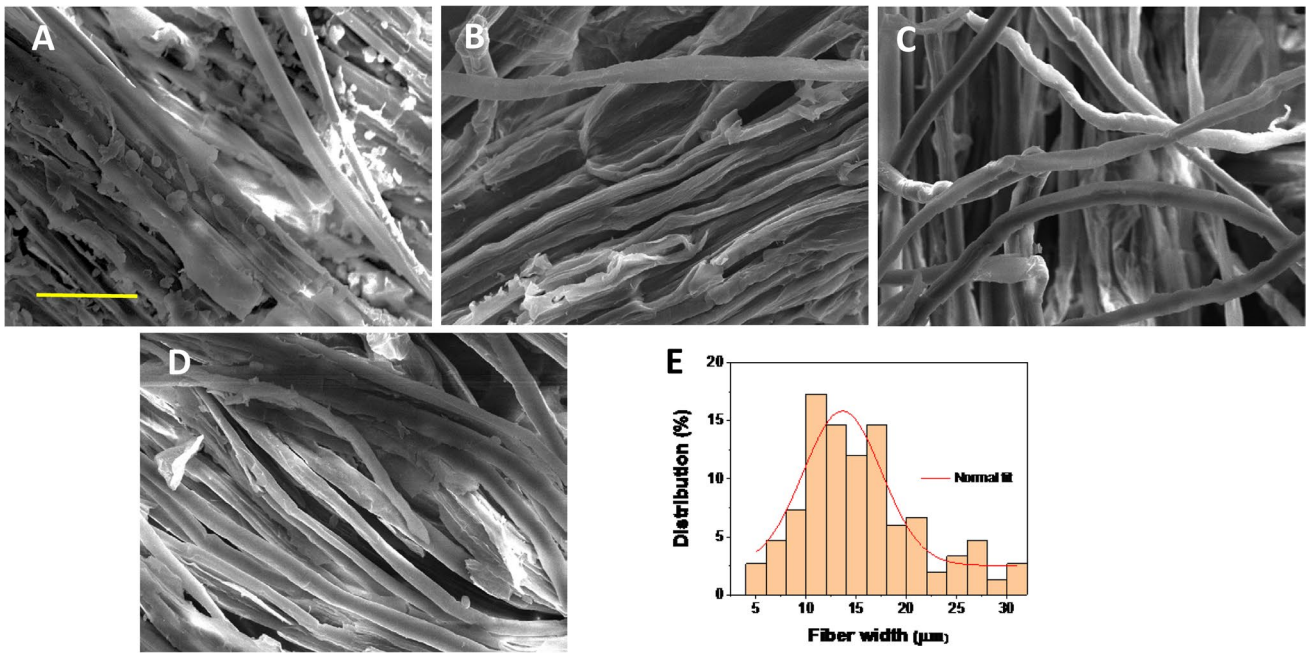


**Fig. 5** SEM images and histogram showing the width of fiber. **A**, **B**, **C**, and **D** Representative SEM images for untreated, 3%, 6%, and 9% treated fiber samples, respectively. A scale bar of 50 μm shown in A also applies for B, C, and D. **E** A histogram plot ($n = 150$ and bin size 2 μm) with a normal distribution fit (solid line) to show the fiber width distribution in %

Literature studies have reported that the water absorption (as measured by % weight gain) depends on the origin (plant source and fiber location) or chemical composition of fiber, treatment condition, and water composition. In majority of studies, alkali-treated sample is reported to have improved water resistance or decreased weight gain [41, 42, 54, 55]. For examples, 1.4 times decrease in % weight gain (from 200 to 140%) was observed in 10% NaOH-treated abaca fiber [55], 2.5 times decrease (from 160 to 65%) was observed in 5% treated *Sterculia* fiber [41], and 1.3 times decrease (from ~ 850 to 630%) in 6% NaOH-treated Areca fiber [56]. Interestingly, increased water absorption is also reported in alkali-treated fiber. For examples, in 6% NaOH-treated cotton ~ 23 times increase (50% in untreated to 1160% in treated) and 1.5 increase in pineapple fiber (200% in untreated to 300% in treated) is reported. It is reasoned that alkali treatment removes hydrophobic waxy layer resulting increase in water uptake [56].

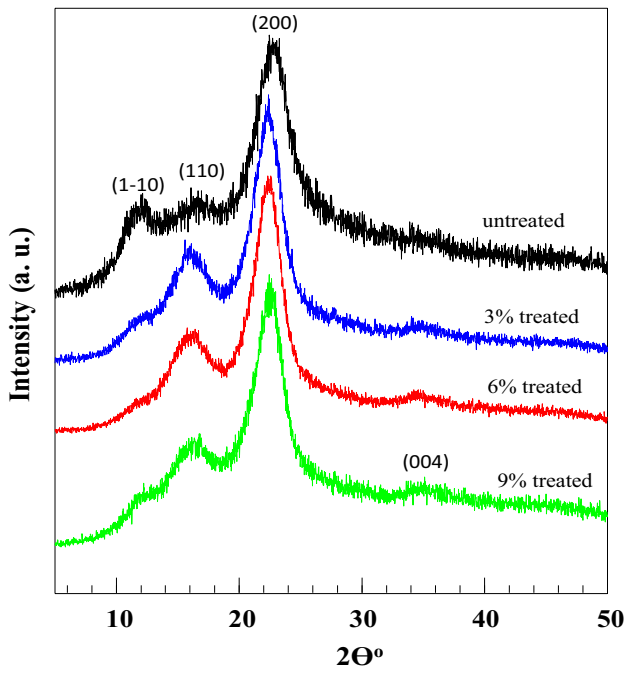


**Fig. 6** XRD data of untreated and alkali-treated samples. For easy composition, data is overlaid vertically. The number within parentheses indicates the crystalline planes

## 3.3 FTIR study

The FTIR spectra of the fiber samples are very similar with a small difference in peak intensity, peak position, and shape of some specific bands (Fig. 4). A broad peak in the range of 3000–3600 $cm^{-1}$ is assigned to the O–H stretching frequency of hydrogen-bonded networks in cellulose and hemicellulose [47, 57]. In alkali-treated samples, the shape of the band becomes more symmetric and narrower. This could be due to the disruption of hydrogen bonding between O–H groups of hemicellulose and cellulose resulting from partial loss of hemicellulose.

**Table 2** XRD parameters for the fiber samples

| Sample type | CI (%) | 2Θ (°) | $d_{200}$ (nm) | $\beta$ (°) | $D$ (nm) |
|---|---|---|---|---|---|
| Untreated | 73 | 22.8 | 0.390 | 3.3 | 2.45 |
| 3% treated | 76.2 | 22.3 | 0.398 | 2.7 | 3.00 |
| 6% treated | 78.5 | 22.4 | 0.396 | 2.7 | 3.00 |
| 9% treated | 75.25 | 22.5 | 0.395 | 2.9 | 2.79 |

A weak peak at 1730 $cm^{-1}$ is attributed to ester or acetyl -C = O groups of (non-conjugated) hemicellulose or lignin [26, 29]. A characteristic peak at ~ 1260 $cm^{-1}$ is attributed to the C-O stretching of acetyl groups of hemicellulose and cellulose [57]. These peaks are weaker in alkali-treated samples indicating removal of hemicellulose and lignin. These spectral changes are consistent with the weight loss data reported in Sect. 3.1. A characteristic peak ~ 1430 $cm^{-1}$ attributed to $-CH_2$ bending vibration remains unchanged in the alkali-treated sample. This intact cellulose could help to preserve mechanical strength in the alkali-treated fiber [47, 58].

### 3.4 SEM imaging

The fiber surface of the untreated sample contains additional materials deposited on the surface (Fig. 5A). The additional mass could be non-cellulosic materials such as pectin, wax, inorganic minerals, hemicellulose, and lignin. Interestingly, in the alkali-treated samples surface impurities are removed and the fiber bundles separate into individual fibers. This observation is also consistent with the weight loss in the retting study, reduction of effective fiber bundle width, and weakening of hemicellulose and lignin-specific peaks in FTIR spectra reported in Sect. 3.1.

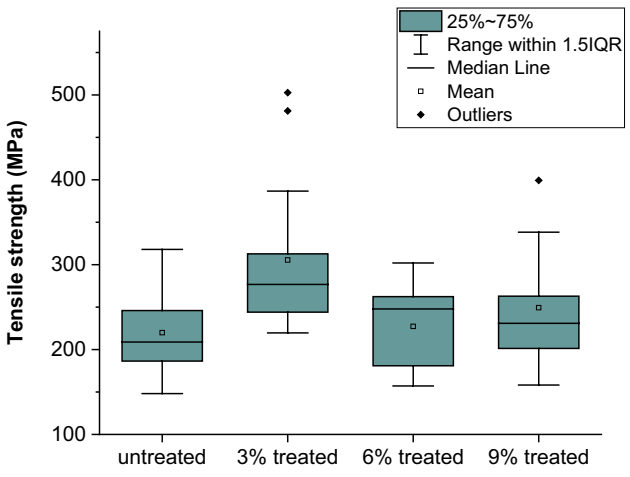


**Fig. 7** Tensile strength data for the fiber samples. For easy comparison, mean, inter-quartile range and median values along with a few outliers ($n = 15$) are shown as a box and Whisker plot

Similar changes were reported in alkali-retted hemp [59], *Sterculia* [12], *Bauhinia* [41], kenaf [60], *M. oleifera* fruit fibers [48], *Carica papaya* bark fibers (5% NaOH [49], and water hyacinth plant fiber [50]. The single elementary fiber mean width and the width range ($n = 150$) measured from the 9% treated sample were found to be 15.4 ± 6 µm and 4.8–31.5 µm, respectively. A histogram plot showing the fiber width distribution is provided in Fig. 5E.

### 3.5 XRD study

The shape of the XRD profile for all the fiber samples resembles to that of a typical lignocellulose fiber (Fig. 6). Cellulose fiber in its natural form contains crystalline and amorphous domains [15, 61, 62]. The diffraction peaks at 2θ value at ~ 13° and ~ 16° originate from the crystalline planes (1–10) and (110), respectively. The strongest peak at ~ 22.5° originates from the (200) plane and a weak peak at ~ 35° from (004) planes of crystalline cellulose phase I, respectively [15, 61, 62]. To get a piece of preliminary information on crystallinity change on alkali retting, Segal's crystallinity index (CI) was calculated using Eq. (5).

$$CI = 100\left(\frac{I_{200}}{I_{200} + I_{am}}\right) \tag{5}$$

where $I_{200}$ and $I_{am}$ are the intensities of major crystalline peak and amorphous profile measured at 2θ values of ~ 22.5° and ~ 18.2°, respectively. The Segal's crystallinity index (CI) in untreated, 3%, 6%, and 9% alkali-treated samples was found to be 73%, 76.2%, 78.5%, and 75.2%, respectively. It is suggested that the removal of amorphous components such as hemicellulose and lignin mainly from the inter-fibrillar region can lead to the reorganization of cellulose chains and the increase in crystallinity index [12, 15, 37, 37, 47]. The same reasoning can explain the CI increase in alkali-treated samples. Increase in CI with alkali treatment is also reported in several other fiber types, for example, *M. oleifera* fruit fibers [48], *Carica papaya* bark fibers [49], water hyacinth fiber [50], and *Sterculia* fiber [12].

The full width at half maximum parameter (β, in radians) corresponding to the most intense peak corresponding to (200) plane was used to get crystallite size (D, nm) using the Scherrer equation [63].

$$D = \frac{\kappa\lambda}{\beta\cos\theta} \tag{6}$$

The $\kappa$ factor of 0.94 and λ of 0.154 nm were used in the calculation. It is found that crystallite size increased by approximately 22% in both 3% and 6% alkali-treated samples and by 14% in the 9% alkali-treated sample (Table 2). The XRD data were further analyzed to get information on inter-planar spacing ($d_{200}$) (Eq. 7).

**Table 3** Comparison of mechanical properties

| Fiber | Treatment conditions | Tensile strength (MPa) | Elongation (%) |
|---|---|---|---|
| Lokta fiber (this study) | 9% NaOH, RT, 1 h | 249.3 ± 32.2 | 6–9 |
| Jute fiber [47] | 8% NaOH, RT, 1 h | 350 ± 32.2 | 1–4 |
| Carica papaya bark fibers [49] | 5% NaOH, RT, 1 h | 548 ± 14.6 | 1.83 ± 0.04 |
| Borassus fruit fiber [37] | 10% NaOH, RT, 0.5 h | 160 | 34 |
| Prosopis juliflora bark fiber [65] | Raw fiber | 558 ± 13.4 | 1.77 ± 0.04 |
| Cotton fiber [66] | Variable | 200–400 | 6–8 |
| Coir [66] | Variable | 95–175 | 13.7–41 |
| Flax [66] | - | 500–1500 | 2.7–3.2 |
| Bamboo fiber [67] | 5% NaOH, RT, 24 h | 222 ± 14.6 | 15.2 ± 0.04 |

$$n\lambda = 2d_{200}\sin\theta \tag{7}$$

In the calculation, $n = 1$ (first order diffraction), $\lambda$ of 0.154 nm was used and θ was obtained from peak position of $d_{200}$ (from XRD data). A small increase in inter-planar spacing ($d_{200}$) in alkali-treated samples could be due to micro-strains present on the crystallite surface [57, 64].

### 3.6 Mechanical strength

The tensile strength (MPa) data for the fiber samples is provided as a Box and Whisker plot (Fig. 7). The tensile strength for untreated, 3%, 6%, and 9% treated samples was found to be 219.9 ± 24.2 MPa, 305.5 ± 44.0 MPa, 227.3 ± 23.3 MPa, and 249.3 ± 32.2 MPa, respectively. The corresponding % elongation was found to be 8.5 ± 1.4, 7.0 ± 1.0, 8.0 ± 1.0, and 8.0 ± 1.1, respectively. This showed that tensile strength increases significantly on alkali treatment ($p < 0.01$). Literature studies report that tensile strength in alkali-treated samples, depending on treatment parameters and fiber type, is increased or decreased on retained [3, 19, 47, 59]. It is suggested that the removal of lignin and hemicellulose mainly from inter-fibrillar region decreases the internal constraint within cellulose chains and facilitates better organization. This could increase the tensile strength. The same reasoning could help to explain the tensile strength increase in Lokta fiber reported here. A small decrease in tensile strength at high alkali concentrations could be due to the formation of fiber surface defects.

The mechanical properties of natural fiber depend on fiber type and treatment conditions. Not all studies report the measurement parameters such as gauge length, testing speed, fiber diameter or width, and temperature and humidity. A comparison with few selected studies, which report very similar treatment conditions as this study, is provided in Table 3.

It is suggested that % elongation increases with microfibril angle (MFA) [65, 68]. For natural fiber, MFA ranges from 3 to 50°. Cotton is reported to have MFA of 20–30°, so it has higher % elongation (6–8%) than flax fiber (% elongation ~ 3%, MFA 10°). Lokta fiber has very similar % elongation as cotton fiber, and the MFA could be similar. It is found that fiber having low MFA and higher cellulose content can have high ultimate tensile strength [69]. The intermediate tensile strength of Lokta fiber could be due to high cellulose content and high MFA. Experimental measurement of microfibril angle, stress–strain curve, and SEM image of fiber surface at different levels of stress could provide more insight to the mechanical properties of the fibers.

### 3.7 Thermal analysis

The TGA and DTG data for selected fiber samples are reported in Fig. 8 and the insets, respectively. The TGA data for all samples show three distinct weight loss regions viz. T < 100 °C, 175–400 °C, and > 400 °C, as reported for

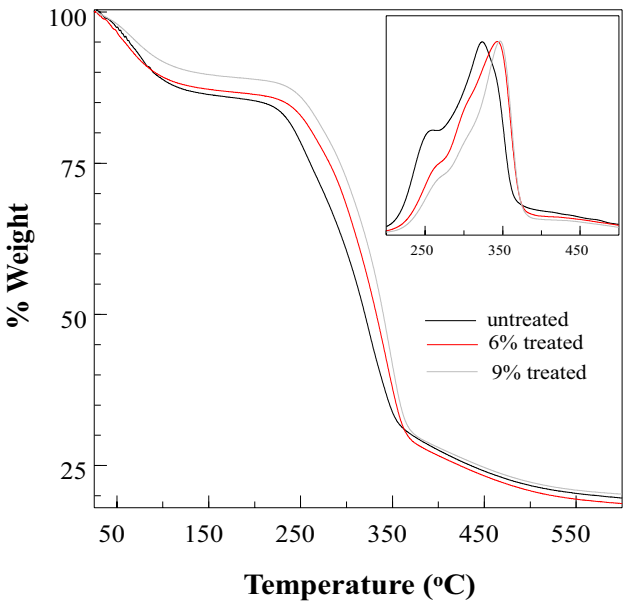


**Fig. 8** Thermal analysis data. The main frame shows the TGA data for untreated, 6%, and 9% NaOH-treated samples. The inset shows the corresponding DTG data

**Table 4** A summary of TGA data

| Sample type | ΔT, °C | Mass loss, % | Maximum degradation temperature ($T_{max}$), °C | Residual mass or char at 600 °C, % |
|---|---|---|---|---|
| Untreated | 26–100 | 11 | 325 | 18.9 |
| | 100–275 | 20 | | |
| | 275–375 | 40 | | |
| | 375–650 | 11.3 | | |
| 6% treated | 26–100 | 10 | 343 | 18.0 |
| | 100–275 | 12.6 | | |
| | 275–375 | 47.5 | | |
| | 375–650 | 10.7 | | |
| 9% treated | 26–100 | 8 | 347 | 19.7 |
| | 100–275 | 9.5 | | |
| | 275–375 | 50.2 | | |
| | 375–650 | 9.8 | | |

typical lignocellulose biomass [48–50, 70]. For easy comparison, the % weight loss in different temperature windows is also provided in Table 4. In all samples, the initial weight at T < 100 °C is due to loss of volatile impurities and moisture. A small difference in weight loss in this region can be due to crystallinity change, differences in chemical composition, and the equilibrium moisture content.

The weight loss in the range of 200–300 °C is mainly due to the degradation of hemicellulose [70]. This region is more pronounced in DTG as a shoulder ~ 260 °C (Fig. 8 inset). Interestingly, the shoulder is stronger in the untreated sample suggesting higher hemicellulose content. This observation is consistent with chemical analysis, FTIR, and SEM data reported in earlier sections. The degradation of hemicellulose at lower temperatures than cellulose is linked to its amorphous nature and ease of de-polymerization [71].

The weight loss in the temperature range of 300–400 °C is mainly attributed to the cleavage of glycosidic linkage in cellulose [71]. This region appears as a sharp peak in DTG. The higher thermal stability of cellulose is due to well-organized long polymeric units. The maximum degradation temperature ($T_{max}$) for untreated, 6% treated, and 9% NaOH-treated samples was found to be 325 °C, 343 °C, and 347 °C, respectively (Table 4). This suggested that thermal stability is increased on alkali treatment. The increased thermal stability on alkali treatment could be linked to increased crystallinity and grain size. Increase in thermal stability on alkali treatment is also reported in other studies, for example increase from 321.1 to 346.6° in *Carica papaya* 5% NaOH-treated (1 h, RT) bark fibers [49] and 321 to 332° in 5% NaOH-treated (4 h, 80 °C) *Sterculia* fiber [12]. These results also indicate that alkali-treated sample has high thermal stability and can be used in the composite materials. Lignin degradation is reported to take place at a broad temperature range from 200 to 600 °C. This is attributed to high molecular mass having cross-linked structure [72]. The higher weight loss in the temperature ranges from 475 to 600 in the untreated sample could be due to higher lignin content.

A small difference is residual mass left could be due to difference in chemical composition and other impurities, for example inorganic minerals present. The residual mass ~ 600 °C is reported to increase or decrease [49] on alkali treatment. It is suggested that removal of hemicellulose can form more stable lignin–cellulose complex, which can result in increased residual char in alkali-treated sample [73]. This could explain an increase in residual char from 18.9% in untreated sample to 19.7% in 9% NaOH-treated sample. The residual mass around 600 °C is reported to be variable, for examples around 40% is reported in raw and alkali-treated *Acacia planifrons* bark fibers [74], 30–40% in raw and alkali-treated *Carica papaya* bark fibers [49], 25–28% in *Sterculia* fiber [12], 15–22% in jute fibers [73], 20–22% in Alfa stem fiber [20], 30–32% in water hyacinth fibers [50]. The low residual mass could suggest that Lokta fiber has low mineral impurities, and the biomass may be easy to process for making paper and biocomposite materials.

## 4 Conclusions

To summarize, several material properties of the untreated and 1%, 3%, 6%, and 9% NaOH-treated (w/v) Lokta fiber samples were systematically explored. The alkali treatment resulted in significant loss of extractives, lignin, and hemicellulose with increasing alkali concentration. This resulted in significant increase in cellulose content (from ~ 37 to 61%) in 9% NaOH-treated sample. The equilibrium moisture content and effective fiber width decreased significantly whereas fiber density, crystallinity index, and thermal stability increased on alkali treatment. These changes are due to the loss of lignin and hemicellulose from the fiber bundle, as shown by the evidence obtained from FTIR data and SEM images. The tensile strength for untreated, 3%, 6%, and 9% NaOH-treated fiber was found to be 219.9 ± 24.2 MPa, 305.5 ± 44.0 MPa, 227.3 ± 23.3 MPa, and 249.3 ± 32.2 MPa;

respectively. This showed that tensile strength increased significantly on alkali treatment ($p < 0.01$). The maximum degradation temperature ($T_{max}$) for untreated, 6% treated, and 9% NaOH-treated samples was found to be 325 °C, 343 °C, and 347 °C; respectively. This suggested that thermal stability is increased on alkali treatment. These findings will be important to optimize and understand the end properties of the Lokta fiber–based paper and composite materials. Experimental measurement of tensile curves and fracture analysis could provide more insight to the mechanical properties of the fibers. Additionally, a systematic study on material properties of Lokta fiber–derived paper and composite materials could be explored in future.

**Acknowledgements** The authors would like to acknowledge Dr. Zhiping Luo from Fayetteville State University for providing IMREL facility and Prof. Dr. Rameshwar Adhikari from Research Centre for Applied Science and Technology (RECAST), Tribhuvan University, Nepal for supporting in FTIR measurement.

**Author contribution** Conceptualization: [Bhanu Bhakta Neupane]; methodology: [Girja Mani Aryal, Krisha Prasad Kandel, Menuka Adhikari, Bhoj Gautam]; formal analysis and investigation: [Girja Mani Aryal, Menuka Adhikari, Hisila Dangol, Madan Poudel, Sushil Pokharel, Jianna Evans, Ramdeep Shrestha]; original draft preparation: [Girja Mani Aryal, Krishna Prasad Kandel]; preparing final paper: [Bhanu Bhakta Neupane, Bhoj Gautam, Menuka Adhikari]; funding acquisition: [Bhanu Bhakta Neupane, Bhoj Gautam]; supervision: [Bhanu Bhakta Neupane, Bhoj Gautam]. All authors have read and agreed to publish the current version of the manuscript.

**Funding** This work was supported by the University Grants Commission, Nepal (BBN # CRIG-78/79-S&T-02) and by National Science Foundation, USA (BG# EES 1900998).

**Data availability** The data that support the findings of this study are available from the corresponding authors [B. B. N and B. G.] upon reasonable request.

## Declarations

**Ethical approval** Not applicable.

**Competing interests** The authors declare no competing interests.

## References

1. Amara C, El Mahdi A, Medimagh R, Khwaldia K (2021) Nanocellulose-based composites for packaging applications. Curr Opin Green Sustain Chem 31:100512
2. Camargo PHC, Satyanarayana KG, Wypych F (2009) Nanocomposites: synthesis, structure, properties and new application opportunities. Mater Res 12:1–39
3. Chandrasekar M, Ishak MR, Sapuan SM et al (2017) A review on the characterisation of natural fibres and their composites after alkali treatment and water absorption. Plast Rubber Compos 46:119–136
4. Dufresne A (2008) Chapter 19 - cellulose-based composites and nanocomposites. In: Belgacem MN, Gandini A (eds) Monomers, Polymers and Composites from Renewable Resources. Elsevier, Amsterdam, pp 401–18
5. Liu W, Du H, Zhang M et al (2020) Bacterial cellulose-based composite scaffolds for biomedical applications: a review. ACS Sustain Chem Eng 8:7536–7562
6. Lobo FC, Franco AR, Fernandes EM, Reis RL (2021) An overview of the antimicrobial properties of lignocellulosic materials. Molecules 26:1749
7. Shavandi A, Hosseini S, Okoro OV et al (2020) 3D bioprinting of lignocellulosic biomaterials. Adv Healthc Mater 9:2001472
8. Sanjay MR, Madhu P, Jawaid M et al (2018) Characterization and properties of natural fiber polymer composites: a comprehensive review. J Clean Prod 172:566–581
9. Vinod A, Sanjay MR, Suchart S, Jyotishkumar P (2020) Renewable and sustainable biobased materials: an assessment on biofibers, biofilms, biopolymers and biocomposites. J Clean Prod 258:120978
10. Jagadeesh P, Puttegowda M, Thyavihalli Girijappa YG et al (2022) Effect of natural filler materials on fiber reinforced hybrid polymer composites: An Overview. J Nat Fibers 19:4132–4147
11. Bismarck A, Mishra S, Lampke T (2005) Plant fibers as reinforcement for green composites. Natural fibers, biopolymers, and biocomposites: CRC Press, pp 52–128
12. Kandel KP, Adhikari M, Kharel M et al (2022) Comparative study on material properties of wood-ash alkali and commercial alkali treated Sterculia fiber. Cellulose 29:5913–5922
13. Ververis C, Georghiou K, Christodoulakis N et al (2004) Fiber dimensions, lignin and cellulose content of various plant materials and their suitability for paper production. Ind Crops Prod 19:245–254
14. Fu S-Y, Lauke B (1996) Effects of fiber length and fiber orientation distributions on the tensile strength of short-fiber-reinforced polymers. Compos Sci Technol 56:1179–1190
15. Park S, Baker JO, Himmel ME et al (2010) Cellulose crystallinity index: measurement techniques and their impact on interpreting cellulase performance. Biotechnol Biofuels 3:1–10
16. Tanpichai S, Sampson WW, Eichhorn SJ (2012) Stress-transfer in microfibrillated cellulose reinforced poly (lactic acid) composites using Raman spectroscopy. Compos Part Appl Sci Manuf 43:1145–1152
17. Obame SV, Betené ADO, Naoh PM et al (2022) Characterization of the Neuropeltis acuminatas liana fiber treated as composite reinforcement. Results Mater 16:100327
18. Betené ADO, Batoum CS, Ndoumou Belinga RL et al (2023) Extraction and characterization of a novel tropical fibre *Megaphrynium macrostachyum* as a biosourced reinforcement for gypsum-based biocomposites. J Compos Mater 57:2543–2562
19. Hashim MY, Amin AM, Marwah OMF et al (2017) The effect of alkali treatment under various conditions on physical properties of kenaf fiber. J Phys Conf Ser 914:012030
20. Borchani KE, Carrot C, Jaziri M (2015) Untreated and alkali treated fibers from Alfa stem: effect of alkali treatment on structural, morphological and thermal features. Cellulose 22:1577–1589
21. Vardhini KJ, Murugan R, Rathinamoorthy R (2019) Effect of alkali treatment on physical properties of banana fibre. Indian J Fibre Text Res IJFTR 44:459–465
22. Km A, Nayeem J, Quadery AH et al (2018) Handmade paper from waste banana fibre. Bangladesh J Sci Ind Res 53:83–88
23. Aryal GM, Ware W, Han S et al (2021) Microscopic characterization of eco-friendly Lokta paper. Microsc Microanal 27:720–721
24. Aryal GM, Kandel KP, Bhattarai RK et al (2022) Material properties of traditional handmade paper samples fabricated from cellulosic fiber of Lokta bushes. ACS Omega 7:32717–32726
25. Elanthikkal S, Gopalakrishnapanicker U, Varghese S, Guthrie JT (2010) Cellulose microfibres produced from banana plant wastes: isolation and characterization. Carbohydr Polym 80:852–859

26. Haque MM, Hasan M, Islam MS, Ali ME (2009) Physico-mechanical properties of chemically treated palm and coir fiber reinforced polypropylene composites. Bioresour Technol 100:4903–4906
27. Booth I, Goodman AM, Grishanov SA, Harwood RJ (2004) A mechanical investigation of the retting process in dew-retted hemp (Cannabis sativa). Ann Appl Biol 145:51–58
28. Obi Reddy K, Uma Maheswari C, Shukla M, Muzenda E (2014) Preparation, chemical composition, characterization, and properties of Napier grass paper sheets. Sep Sci Technol 49:1527–1534
29. Tanpichai S, Witayakran S, Srimarut Y et al (2019) Porosity, density and mechanical properties of the paper of steam exploded bamboo microfibers controlled by nanofibrillated cellulose. J Mater Res Technol 8:3612–3622
30. Jabbari F, Babaeipour V, Bakhtiari S (2022) Bacterial cellulose-based composites for nerve tissue engineering. Int J Biol Macromol 217:120–130
31. Tanpichai S, Boonmahitthisud A, Soykeabkaew N, Ongthip L (2022) Review of the recent developments in all-cellulose nanocomposites: properties and applications. Carbohydr Polym 286:119192
32. Torres FG, Arroyo JJ, Troncoso OP (2019) Bacterial cellulose nanocomposites: an all-nano type of material. Mater Sci Eng C 98:1277–1293
33. Sitotaw YW, Habtu NG, Gebreyohannes AY et al (2021) Ball milling as an important pretreatment technique in lignocellulose biorefineries: a review. Biomass Convers Biorefinery. https://doi.org/10.1007/s13399-021-01800-7
34. Humphrey J, Navas-Alemán L (2010) Value chains, donor interventions and poverty reduction: a review of donor practice. IDS Research report 63. https://www.ids.ac.uk/download.php?file=files/dmfile/rr63.pdf. Accessed Jan 2024
35. Biggs S, Messerschmidt D (2005) Social responsibility in the growing handmade paper industry of Nepal. World Dev 33:1821–1843
36. Government of Nepal (2017) Nepal national center export strategy: handmade paper and paper products 2017–2021. International trade center, Government of Nepal, https://moics.gov.np/public/uploads/shares/strategy/Handmade_Paper__Paper_Products_compressed.pdf. Accessed Jan 2024
37. Boopathi L, Sampath PS, Mylsamy K (2012) Investigation of physical, chemical and mechanical properties of raw and alkali treated Borassus fruit fiber. Compos Part B Eng 43:3044–3052
38. Van de Weyenberg I, Truong TC, Vangrimde B, Verpoest I (2006) Improving the properties of UD flax fibre reinforced composites by applying an alkaline fibre treatment. Compos Part Appl Sci Manuf 37:1368–1376
39. Das AM, Ali AA, Hazarika MP (2014) Synthesis and characterization of cellulose acetate from rice husk: eco-friendly condition. Carbohydr Polym 112:342–349
40. Adeeyo OA, Oresegun OM, Oladimeji TE (2015) Compositional analysis of lignocellulosic materials: evaluation of an economically viable method suitable for woody and non-woody biomass. Am J Eng Res AJER 4:14–19
41. Kandel KP, Aryal GM, Neupane BB (2023) Kinetics of water sorption in single Sterculia and Bauhinia fibers at ambient temperature. Results Chem 5:100872
42. Espert A, Vilaplana F, Karlsson S (2004) Comparison of water absorption in natural cellulosic fibres from wood and one-year crops in polypropylene composites and its influence on their mechanical properties. Compos Part Appl Sci Manuf 35:1267–1276
43. Beakou A, Ntenga R, Lepetit J et al (2008) Physico-chemical and microstructural characterization of "Rhectophyllum camerunense" plant fiber. Compos Part Appl Sci Manuf 39:67–74
44. Truong M, Zhong W, Boyko S, Alcock M (2009) A comparative study on natural fibre density measurement. J Text Inst 100:525–529
45. ASTM (2004) ASTM D1776–04. American Society for Testing and Materials, West Conshohocken, Pennsylvania, USA, Standard practice for conditioning and testing textiles
46. Elmogahzy Y, Farag R (2018) Chapter 7-Tensile properties of cotton fibers: Importance, research, and limitations. In: Bunsell AR, editor. Handbook of Properties of Textile and Technical Fibers (Second Edition): Woodhead Publishing, p 223–273
47. Saha P, Manna S, Chowdhury SR et al (2010) Enhancement of tensile strength of lignocellulosic jute fibers by alkali-steam treatment. Bioresour Technol 101:3182–3187
48. Bharath KN, Madhu P, Gowda TGY et al (2020) Alkaline effect on characterization of discarded waste of Moringa oleifera fiber as a potential eco-friendly reinforcement for biocomposites. J Polym Environ 28:2823–2836
49. Saravanakumaar A, Senthilkumar A, Saravanakumar SS et al (2018) Impact of alkali treatment on physico-chemical, thermal, structural and tensile properties of *Carica papaya* bark fibers. Int J Polym Anal Charact 23:529–536
50. Sumrith N, Techawinyutham L, Sanjay MR et al (2020) Characterization of alkaline and silane treated fibers of 'water hyacinth plants' and reinforcement of 'water hyacinth fibers' with bioepoxy to develop fully biobased sustainable ecofriendly composites. J Polym Environ 28:2749–2760
51. Mwaikambo LY, Ansell MP (2002) Chemical modification of hemp, sisal, jute, and kapok fibers by alkalization. J Appl Polym Sci 84:2222–2234
52. Aziz SH, Ansell MP (2004) The effect of alkalization and fibre alignment on the mechanical and thermal properties of kenaf and hemp bast fibre composites: Part 1–polyester resin matrix. Compos Sci Technol 64:1219–1230
53. Modibbo UU, Aliyu BA, Nkafamiya II (2009) The effect of mercerization media on the physical properties of local plant bast fibres. Int J Phys Sci 4:698–704
54. Gouanvé F, Marais S, Bessadok A et al (2007) Kinetics of water sorption in flax and PET fibers. Eur Polym J 43:586–598
55. Punyamurthy R, Sampathkumar D, Srinivasa CV, Bennehalli B (2012) Effect of alkali treatment on water absorption of single cellulosic abaca fiber. BioResources 7:3515–3524
56. Begum HA, Tanni TR, Shahid MA (2021) Analysis of water absorption of different natural fibers. J Text Sci Technol 7:152–160
57. Sinha E, Rout SK (2008) Influence of fibre-surface treatment on structural, thermal and mechanical properties of jute. J Mater Sci 43:2590–2601
58. Sui G, Fuqua MA, Ulven CA, Zhong WH (2009) A plant fiber reinforced polymer composite prepared by a twin-screw extruder. Bioresour Technol 100:1246–1251
59. Liu H, You L, Jin H, Yu W (2013) Influence of alkali treatment on the structure and properties of hemp fibers. Fibers Polym 14:389–395
60. Fiore V, Di Bella G, Valenza A (2015) The effect of alkaline treatment on mechanical properties of kenaf fibers and their epoxy composites. Compos Part B Eng 68:14–21
61. French AD (2020) Increment in evolution of cellulose crystallinity analysis. Cellulose 27:5445–5448
62. Yao W, Weng Y, Catchmark JM (2020) Improved cellulose X-ray diffraction analysis using Fourier series modeling. Cellulose 27:5563–5579
63. Cullity B (1978) Elements of X-ray diffraction. Addision wisely Publishing Company Inc., London
64. Ioelovich M (2018) Determination of distortions and sizes of cellulose nanocrystallites. Res J Nanosci Eng 2:1–5
65. Saravanakumar SS, Kumaravel A, Nagarajan T et al (2013) Characterization of a novel natural cellulosic fiber from Prosopis juliflora bark. Carbohydr Polym 92:1928–1933
66. Seki Y, Sever K, Erden S et al (2012) Characterization of *Luffa cylindrica* fibers and the effect of water aging on the mechanical

properties of its composite with polyester. J Appl Polym Sci 123:2330–2337
67. Wong KJ, Yousif BF, Low KO (2010) The effects of alkali treatment on the interfacial adhesion of bamboo fibres. Proc Inst Mech Eng Part J Mater Des Appl 224:139–148
68. Reddy N, Yang Y (2005) Structure and properties of high quality natural cellulose fibers from cornstalks. Polymer 46:5494–5500
69. Petroudy SD (2017) Chapter 3-Physical and mechanical properties of natural fibers. In: Fan M, Fu F (eds) Advanced high strength natural fibre composites in construction. Woodhead Publishing, pp 59–83
70. Poletto M, Ornaghi HL, Zattera AJ (2014) Native cellulose: structure, characterization and thermal properties. Materials 7:6105–6119
71. Yang H, Yan R, Chen H et al (2006) In-depth investigation of biomass pyrolysis based on three major components: hemicellulose, cellulose and lignin. Energy Fuels 20:388–393
72. Kim H-S, Kim S, Kim H-J, Yang H-S (2006) Thermal properties of bio-flour-filled polyolefin composites with different compatibilizing agent type and content. Thermochim Acta 451:181–188
73. Ray D, Sarkar BK, Basak RK, Rana AK (2002) Study of the thermal behavior of alkali-treated jute fibers. J Appl Polym Sci 85:2594–2599
74. Senthamaraikannan P, Saravanakumar SS, Sanjay MR et al (2019) Physico-chemical and thermal properties of untreated and treated Acacia planifrons bark fibers for composite reinforcement. Mater Lett 240:221–224